Synchronization in the human cardiorespiratory system

Carsten Schäfer,[1,*] Michael G. Rosenblum,[1,†] Hans-Henning Abel,[2] and Jürgen Kurths[1]
[1]*Department of Physics, Potsdam University, Am Neuen Palais 10, Postfach 601553, D-14415 Potsdam, Germany*
[2]*Department of Cardioanesthesiology, Städtisches Klinikum Braunschweig, Braunschweig, Germany*
(Received 17 December 1998)

We investigate synchronization between cardiovascular and respiratory systems in healthy humans under free-running conditions. For this aim we analyze nonstationary irregular bivariate data, namely, electrocardiograms and measurements of respiratory flow. We briefly discuss a statistical approach to synchronization in noisy and chaotic systems and illustrate it with numerical examples; effects of phase and frequency locking are considered. Next, we present and discuss methods suitable for the detection of hidden synchronous epochs from such data. The analysis of the experimental records reveals synchronous regimes of different orders $n:m$ and transitions between them; the physiological significance of this finding is discussed.
[S1063-651X(99)12407-3]

PACS number(s): 87.19.Hh, 87.17.Aa, 05.45.−a

I. INTRODUCTION

A well-known common feature of oscillatory systems and biological oscillators, in particular, is their ability to synchronize. Entrainment of periodic (also noisy) self-sustained oscillators by external periodic force, or mutual synchronization of several such oscillators is well understood [1–5], and this theoretical knowledge is widely used in experimental studies and in the modeling of interaction between different physiological (sub)systems. The examples range from the modeling of the heart in the pioneering paper of van der Pol and van der Mark [6] to investigation of the circadian rhythm [7,5], phase locking of respiration with mechanical ventilator [8] or with locomotory rhythms [9], coordinated movement [5] and animal gaits [10], phase locking of chicken embryonic heart cells with external stimuli and interaction of sinus node with ectopic pacemakers [5], synchronization of oscillations of human insulin secretion and glucose infusion [11], locking of spiking from electroreceptors of a paddlefish to weak external electromagnetic field [12], and synchronization of heart rate by external audio or visual stimuli [13]. In the experimental studies, the respective rhythms were usually treated as noise-perturbed periodic oscillations, and phase locking was approximately detected via visual inspection of the experimental data, or by means of phase density histograms [14].

In this paper we use our recent achievements in understanding hidden synchronization effects in chaotic and noisy oscillators [15–19] to address the interaction between cardiovascular and respiratory systems in humans. Although it is well-known that these systems do not act independently [20] and in spite of early communications in the medical literature (that often used different terminology) [21–23], in the biological physics community these two systems were often considered to be not synchronized. So, an extensive review of previous studies of biological rhythms led to the conclusion that ''there is comparatively weak coupling between respiration and the cardiac rhythm, and the resulting rhythms are generally not phase locked'' (see [5], p. 136). Recently, the interaction of these vital systems attracted the attention of several physics groups, and synchronization during paced respiration [24–26] was investigated. Here, as well as in Refs. [21–23] only synchronous states of orders $n:1$ (n heartbeats within 1 respiratory cycle) were found due to limitation of the *ad hoc* methods used for the analysis of data.

In our previous work [27] we have reported on cardiorespiratory synchronization under free-running conditions; the proposed analysis technique allows us to find out synchronous epochs of different orders $n:m$. This finding gives some indication for the existence of an unknown form of cardiorespiratory interaction.

Here we systematically study cardiorespiratory synchronization from the nonlinear dynamics viewpoint. We discuss the difference between this effect and frequency modulation of the heart rhythm known as respiratory sinus arrhythmia (RSA) [28]. Conceptual models are used to demonstrate the notion of synchronization in noisy systems, effects of phase and frequency locking are discussed, and different techniques for quantitative analysis of phase synchronization from experimental data are presented.

The paper is organized as follows. In Sec. II we briefly present the physiological background and describe the experiments performed and the data measured. Section III contains basic notions of synchronization in noisy and chaotic systems illustrated by numerical examples. In Sec. IV we discuss the synchronization approach to the analysis of bivariate data and introduce several techniques for such analysis. Section V presents the results of application of these methods to our data. Finally, in Sec. VI we discuss our results.

II. EXPERIMENT AND PHYSIOLOGICAL BACKGROUND

We performed noninvasive examinations with eight healthy volunteers (14 to 17 years, high performance swimmers, 4 male, 4 female, cf. Table I). The subjects were laying

*Present address: Centre for Nonlinear Dynamics, Department of Physiology, McGill University, 3655 Drummond Street, Montreal, Quebec, Canada H3G 1Y6.
†Author to whom correspondence should be addressed. URL: www.agnld.uni-potsdam.de~/mros

TABLE I. List of subjects: the variability of the interbeat intervals and respiratory cycle length is quantified by the median and the interquartile range (IQR) (difference between first and third quartile) of respective distributions.

			R-R (s)		Respiratory cycle (s)	
Code	Sex	Age	Median	IQR	Median	IQR
A	m	16.1	1.104	0.028	3.110	0.390
B	m	14.6	1.018	0.095	3.210	0.610
C	m	13.9	0.975	0.110	3.230	0.850
D	f	15.2	1.157	0.157	2.930	0.780
E	m	16.9	1.026	0.089	3.650	0.620
F	f	15.0	1.024	0.143	2.960	0.700
G	f	15.9	0.733	0.070	5.615	1.550
H	f	16.3	1.256	0.197	4.260	2.100

at rest and no constraints like paced respiration or mental exercising were used.

The electrocardiogram (ECG) was registered by standard leads and respiration was measured by a thermistor at the nose synchronously, while respiratory abdominal movements were registered for control. The duration of each record is 30 minutes. All signals were digitized with 1000-Hz sampling rate and 12-bit resolution.

For the analysis of the heart rate the times of R peaks in the ECG [Fig. 1(a)] were extracted by a semiautomatic algorithm with manual correction. Only data sets without extrasystoles are used for the subsequent analysis.

The respiratory signals are narrow banded [Fig. 1(b)]; all these records were visually inspected and, if required, preprocessed. After low-frequency trend elimination, a second-order Savitzky-Golay filter [29] was applied to remove high-frequency noise.

Both respiration and heart rate display strong variability; this can be seen from the distributions of the length of respiratory and cardiac cycles (Fig. 2). Both rhythms are typically irregular and strongly nonstationary, as is illustrated in Fig. 3, where the data for one of the subjects are shown.

The human cardiovascular and respiratory systems do not act independently; their interrelation is rather complex and still remains a subject of physiological research (see, e.g., [20,30] and references therein). As a result of this interaction, in healthy subjects the heart rate normally increases during inspiration and decreases during expiration, i.e., the heart rate is modulated by a respiratory-related rhythm. This frequency modulation of the heart rhythm (see Fig. 4) has been known for at least a century and is commonly referred to as RSA. It is well-studied (see, e.g., [31]) and is thought to be due to the following mechanisms: reflection of respiratory blood pressure waves via baroreceptor feedback loop in the heart rate [32], respiratory phase-dependent modulation of baroreflex information processing [33], and central coupling between respiratory neurons on the one hand, and sympathetic and/or parasympathetic neurons on the other hand [34].

The interaction between the cardiovascular system and respiration involves a large number of feedback and feedforward mechanisms. As a first approximation one can regard this coupling as unidirectional, i.e., consider only the influence of the respiratory-related rhythms on the heart rate [20,30]. It is very important to mention that although this arrhythmia (RSA) is termed ''respiratory,'' the variation of the heart rate is not directly caused by respiration itself. Moreover, ''periodic changes in the baroreflex efficiency in this frequency range continue without respiration. This means that this fluctuation of reflex efficiency is not a simple

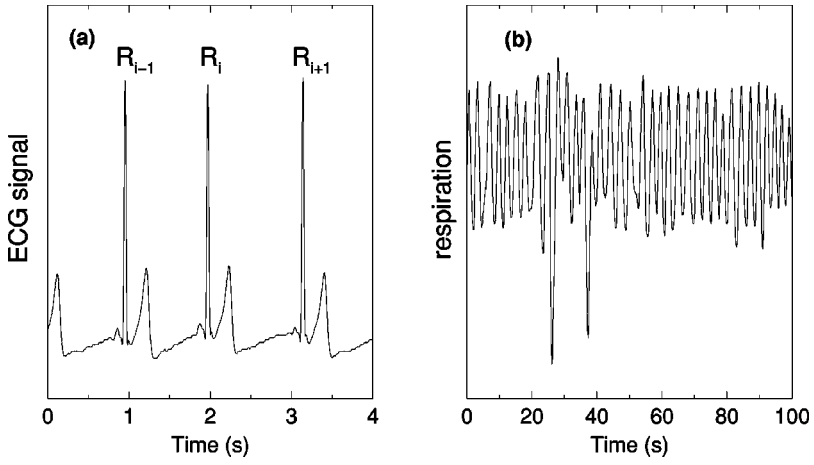

FIG. 1. Short segments of an electrocardiogram with the R peaks marked (a) and of a respiratory signal (b); both signals are in arbitrary units.

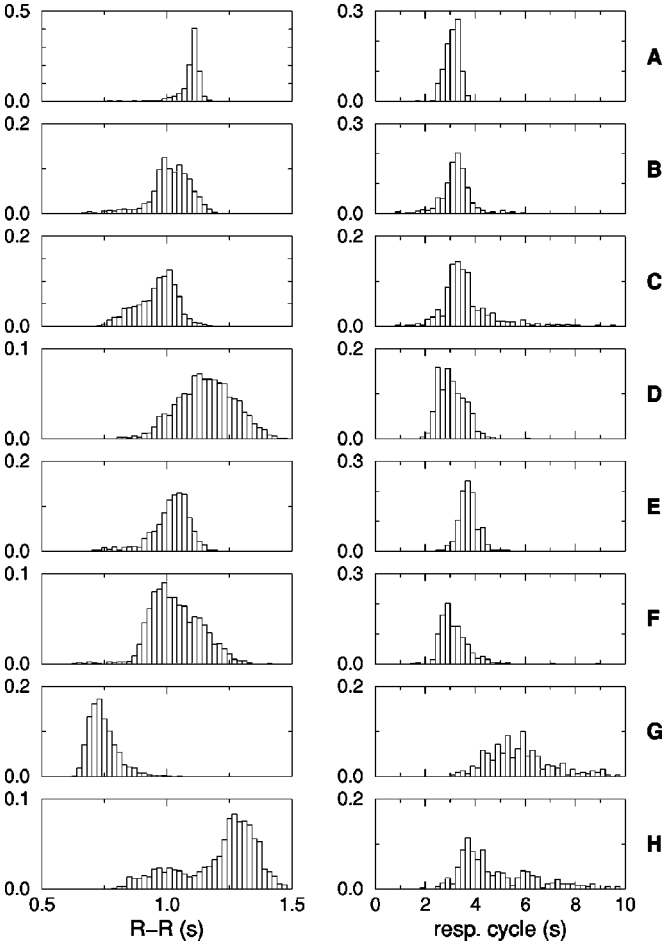

FIG. 2. Distributions of the length of interbeat, or R-R intervals (left panels) and respiratory cycles (right panels) for 1800-s-long measurements demonstrate high variability of both rhythms and strong interindividual differences. The letters to the right of the plots correspond to the subjects codes (cf. Table I).

'irradiation' of a 'respiratory' rhythm generator but rather the expression of an independent rhythm. In most cases the latter is synchronized with the central rhythm, which projects onto the respiratory muscles'' ([20], see also, [35,33]). In other words, there probably exists an additional central generator producing rhythm in the respiratory frequency range [24]. This conjecture is very important in the context of investigation of cardiorespiratory interaction. Analyzing our data and searching for synchronization, we should have in mind that the cardiovascular system may be influenced by *two rhythms* with close or coinciding frequencies. The exact form of this influence is unknown, but it is important that this action is modulating the heart rate, i.e., at least one of these rhythms acts on the cardiovascular system parametrically.

III. SYNCHRONIZATION OF IRREGULAR OSCILLATORS

Synchronization is a universal phenomenon that occurs due to the coupling of two or more nonlinear oscillators. A number of quite different effects are referred to as synchronization. Understood in a wide sense as the mutual time conformity of two or more processes [3,36], this phenomenon lacks a unique definition and requires more precise description in particular cases. For example, in the context of the

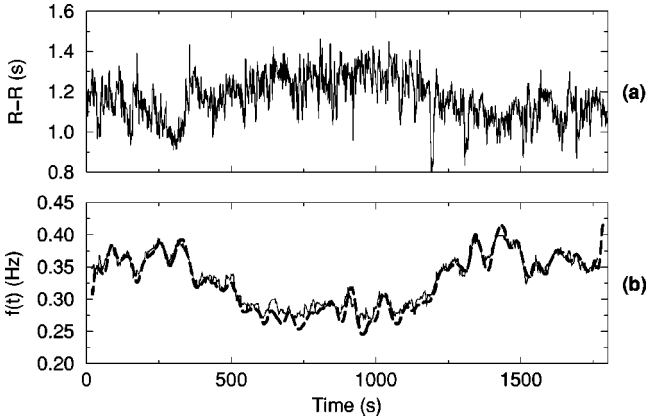

FIG. 3. Nonstationarity of the data (subject D) is demonstrated by strong variability of the R-R (interbeat) intervals (a) and of the instantaneous frequency $f(t)$ of respiration (b). $f(t)$ is calculated by means of two methods. The solid line shows the frequency that corresponds to the maximum of the power spectrum computed in a running window via autoregressive technique (Burg method [29]); window length is 30 s. The dashed line represents the instantaneous frequency obtained with the help of the analytical signal approach (see Appendix A).

interaction of chaotic oscillators one distinguishes between complete, generalized, phase and lag synchronization (see, e.g., [17]), with all these states being defined in different ways.

Throughout this paper we understand synchronization as an adjustment of rhythms of *nonidentical* self-sustained oscillators (or, of the rhythm of one oscillator and that of an external force), due to interaction [36,4]. In the simplest case of two periodic oscillators, synchronization is classically understood as *phase locking*,

$$|\varphi_{n,m}| = |n\phi_1 - m\phi_2| < \text{const}, \tag{1}$$

where n and m are some integers that describe the locking ratio, $\phi_{1,2}$ are the phases of the oscillators, and $\varphi_{n,m}$ is the *generalized phase difference*, or relative phase [37]. Note that the phases $\phi_{1,2}$ are not cyclic on the interval $[0,2\pi]$, but are defined on the whole real line. For periodic oscillators the

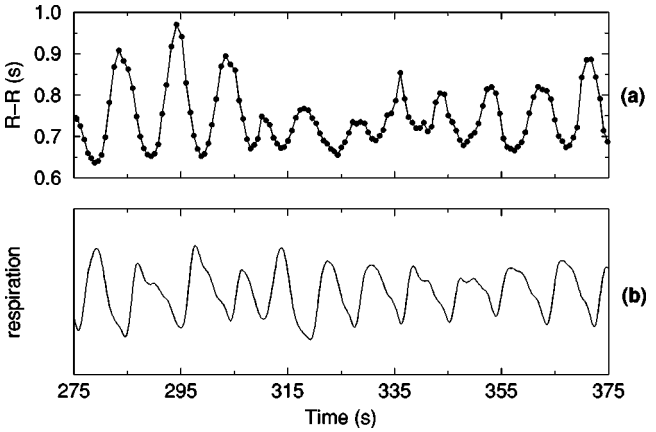

FIG. 4. An example of pronounced respiratory sinus arrhythmia (subject G): heart rate (a) is modulated by a respiratory related rhythm. Respiratory signal (arbitrary units) is shown in (b).

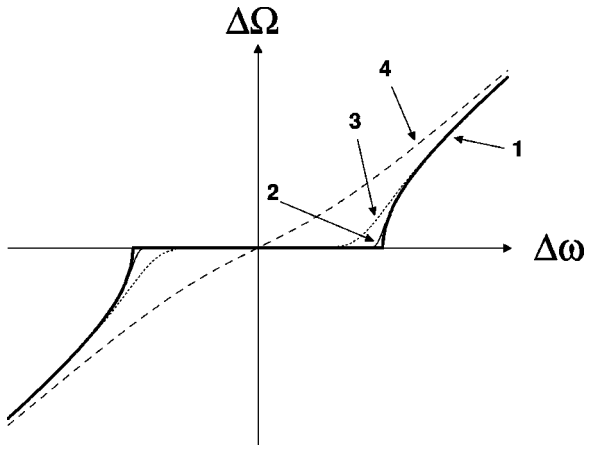

FIG. 5. Qualitative dependence of the frequency difference $\Delta\Omega$ of two coupled periodic oscillators on the parameter mismatch $\Delta\omega$. Curve 1 sketches the noise-free case where the synchronization region can be clearly determined. With an increasing level of noise (curves 2 and 3) the border of synchronization region becomes smeared and then shrinks to a point (curve 4).

condition of phase-locking (1) is equivalent to the condition of *frequency locking* $n\Omega_1 = m\Omega_2$ where $\Omega_{1,2} = \langle \dot{\phi}_{1,2} \rangle$ and brackets mean time averaging. The locking region appears then as a plateau in the plot of $\Delta\Omega = n\Omega_1 - m\Omega_2$ versus the difference $\Delta\omega$ of the parameters that govern the detuning of uncoupled systems (Fig. 5). In other words, if the frequency of one oscillator varies, the second one follows this variation. This adjustment of oscillator frequencies takes place in a certain range of $\Delta\omega$. From the family of curves $\Delta\Omega = f_\varepsilon(\Delta\omega)$ for different strength ε of coupling between oscillators, one can determine the synchronization regions, or Arnold tongues, in the plane $(\Delta\omega, \varepsilon)$.

If we encounter more complicated cases than the interaction of two periodic oscillators, e.g., consider synchronization in the presence of noise, synchronization of chaotic systems, or synchronization of an oscillator with modulated natural frequency, the notion of synchronization becomes essentially less trivial. Moreover, the notions of phase and frequency locking may not be equivalent any more. In the following we illustrate this with several numerical examples.

A. Synchronization as phase locking

First we discuss synchronization in *noisy* periodic oscillators, see, e.g., [2,38,39]. If noise is weak, then in the synchronous state, i.e., in the vicinity of the center of the synchronization region, the generalized phase difference $\varphi_{n,m}$ fluctuates in a random way around some constant value. If the noise is weak and *bounded*, then there exists a range of mismatch $\Delta\omega$, where the condition of frequency locking is fulfilled on average, i.e., $n\langle\Omega_1\rangle = m\langle\Omega_2\rangle$. Near the boundaries of the Arnold tongue, noise can cause *phase slips*, i.e., an ''additional'' or ''missing'' cycle of an oscillator resulting in a rapid upward or downward jump of $\varphi_{n,m}$ by 2π. As a result, the frequency-locking condition is violated, and the transition out of the synchronous regime is now smeared (Fig. 5). If the noise is unbounded, e.g., Gaussian, the probability of a slip to occur is nonzero for $\Delta\omega \neq 0$, so that strictly speaking the synchronization region shrinks to a point. As this probability is (exponentially) small for weak noise, the synchronization region practically appears as an interval of $\Delta\omega$, where $n\langle\Omega_1\rangle \approx m\langle\Omega_2\rangle$. Strong noise can quite often cause phase slips, so that the dependence of the frequency difference $\Delta\Omega$ on the mismatch $\Delta\omega$ is now completely smeared (Fig. 5, curve 4), and, hence, synchronization appears only as a tendency.

Due to phase slips, the question ''synchronous or nonsynchronous'' cannot be answered unambiguously, but only treated in a statistical sense. Following the basic work of Stratonovich [2], we understand phase locking in noisy systems as the appearance of a peak in the *distribution of the cyclic relative phase*

$$\Psi_{n,m} = \varphi_{n,m} \bmod 2\pi. \tag{2}$$

One can interpret this in the following way: There exists a preferred stable value φ_0 of the phase difference between the two oscillators. Under the influence of noisy perturbations this difference either fluctuates around φ_0 or jumps to a physically equivalent stable state $\varphi_0 \pm 2\pi \cdot i$, where i is an integer, and fluctuates around this new stable value, until the next jump occurs. Although due to these noise-induced jumps the phase difference performs a (biased or unbiased) random-walk-like motion; the analysis of the distribution of this cyclic relative phase reveals the existence of a certain preferred value. We can then use the test for deviation of this distribution from the uniform one to quantify synchronization (see [40]).

Before proceeding with numerical illustrations, we mention that our recent studies [15–19] of synchronization of chaotic oscillators have shown that the notion of phase can be introduced for this case as well [41], and effects of phase and frequency locking can be observed, while the amplitudes remain chaotic and, in general, uncorrelated. In particular, it was shown that phase dynamics of chaotic oscillators is qualitatively similar to that of noisy periodic oscillators with chaotic amplitudes playing the role of a noisy perturbation to phases [16]. Depending on the phase-coherence properties of a strange attractor, i.e., on the certain characteristics of the intrinsic ''noise'' in the system, the synchronization properties of a chaotic oscillator are similar to that of a periodic oscillator with a different level of noise. For example, for the Rössler system, the dependence of $\Delta\Omega = \langle \dot{\phi}_1 \rangle - \langle \dot{\phi}_2 \rangle$ looks like the bold curve in Fig. 5, while for the Lorenz system it is like the dotted one [16]. As a consequence of this similarity in the phase dynamics, we can consider synchronization of noisy periodic and chaotic systems from a common viewpoint.

To illustrate the statistical understanding of phase locking, we consider a periodically driven van der Pol oscillator in the presence of noise,

$$\ddot{x} - \mu(1 - x^2)\dot{x} + \omega_0^2 x = \varepsilon \sin(\nu t) + \xi, \tag{3}$$

where $\mu = 1$, the natural frequency $\omega_0 = 1$, and ξ is Gaussian delta-correlated noise, $\langle \xi(t)\xi(t') \rangle = 2D\delta(t - t')$, $D = 0.1$. By varying the frequency ν and amplitude ε of the external force, we look for synchronization of the oscillator by external force. Having in mind the physiological system we are

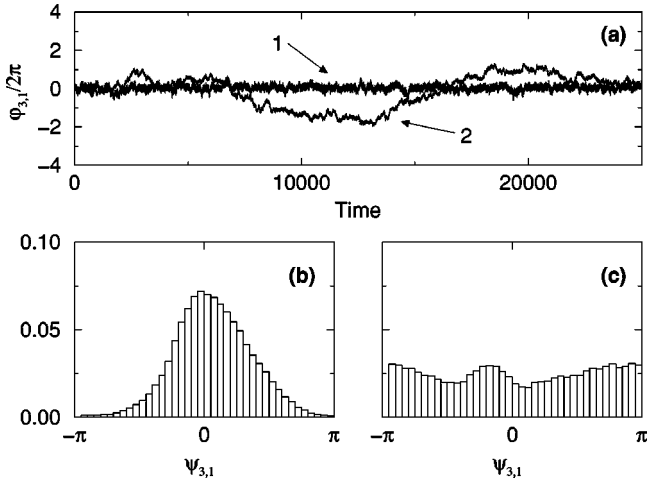

FIG. 6. Phase locking in a noisy oscillator. (a) The phase is locked to that of external force but fluctuates due to noise (curve 1). The distribution of the cyclic relative phase (b) has a pronounced maximum that means existence of a preferred value of the phase difference. Curve 2 in (a) shows an example of coincidence of average frequencies of two uncoupled systems; the absence of synchronization can be seen from the distribution of the cyclic relative phase that is practically uniform (c).

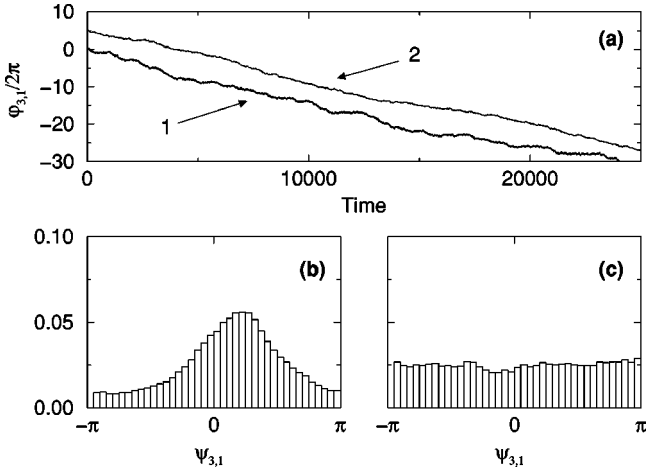

FIG. 7. Statistical phase locking without frequency locking in noisy oscillator. (a) Curves 1 and 2 show the relative phase for the synchronized oscillator and for the case of two uncoupled systems having the same difference of average frequencies, respectively. These cases can be easily distinguished from the distribution of the cyclic relative phase, which is unimodal in the presence of synchronization (b) and fairly uniform otherwise (c).

going to investigate, we have chosen an example of 3:1 locking [42]. To detect synchronization, we compute the phase difference $\varphi_{3,1}=3\nu t-\phi_{vdP}$, where ϕ_{vdP} is the phase of the oscillator.

First we demonstrate the case of unbiased random-walklike motion of the relative phase [Fig. 6(a), curve 1]; the parameters of the external forcing are $\nu=0.287$ and $\varepsilon=0.8$. The phase difference is bounded, so that phase locking in the sense of Eq. (1), as well as frequency locking takes place; the distribution of the cyclic relative phase shows a clear maximum [Fig. 6(b)]. For comparison we show the phase difference of the autonomous oscillator and the periodic force having the same average frequency [Fig. 6(a), curve 2]; the parameters are $\nu=0.3118$ and $\varepsilon=0$. In this way we imitate the occasional coincidence of frequencies. Indeed, the frequency locking seems to be present, although it is destroyed even by the slightest detuning, e.g., if ν changes in the fourth digit. Nevertheless, this case can be easily distinguished from synchronization (curve 1) by means of the distribution of the cyclic relative phase, which is almost uniform [Fig. 6(c)].

Now we examine synchronization of the van der Pol oscillator near the border of the synchronization region; the parameters of forcing are $\nu=0.292$ and $\varepsilon=0.8$. In this case we observe biased random-walk-like motion of the relative phase [Fig. 7(a), curve 1]. The phase difference is unbounded, i.e., there is no frequency locking. Nevertheless, statistically understood phase locking is clearly seen from the distribution of the cyclic relative phase [Fig. 7(b)]. Again, we show for comparison the phase difference in the case of ''occasional'' coincidence of frequencies of autonomous oscillator and external force [$\nu=0.3145$ and $\varepsilon=0$, Fig. 7(a), curve 2]; the distribution of the cyclic relative phase clearly shows the absence of synchronization [Fig. 7(c)]. Similar results for mutually coupled noisy chaotic (Rössler) oscillators are presented in [40,43].

B. Synchronization as frequency locking

In this section we analyze synchronization of a noisy van der Pol oscillator with modulated natural frequency

$$\ddot{x}-\mu(1-x^2)\dot{x}+(\omega_0+\mathcal{F})^2x=\xi, \tag{4}$$

where $\mathcal{F}$ is the modulating term; $\mu=1, \omega_0=1, D=0.05$. Synchronization by parametric action has, to our knowledge, not been studied in the literature. We do not perform a detailed study of this case here, but only report several important properties.

First we consider *periodic modulation* of the natural frequency, $\mathcal{F}=\varepsilon \sin \nu t$, and compute the dependence of the *averaged* frequency of the van der Pol oscillator $\Omega=\langle \dot{\phi}_{vdP}\rangle$ on the modulating frequency ν; this frequency locking is demonstrated in Fig. 8, curve 1, for $\varepsilon=0.6$. In contrast to the case of synchronization by additive forcing, this locking oc-

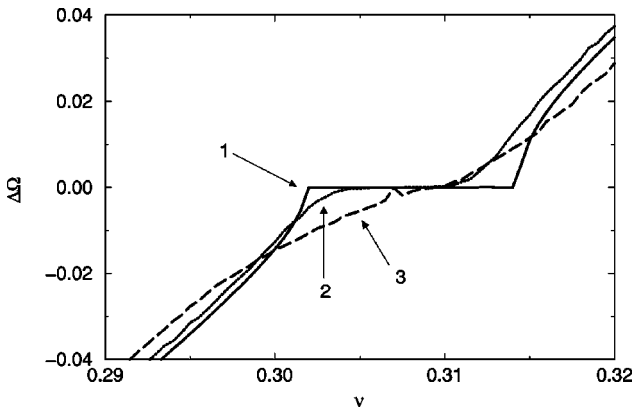

FIG. 8. Synchronization of a van der Pol oscillator via harmonic modulation of its natural frequency (curve 1). The borders of the synchronization region are smeared in the presence of noise (curve 2), or noise and second, low-amplitude, harmonic modulating force (curve 3).

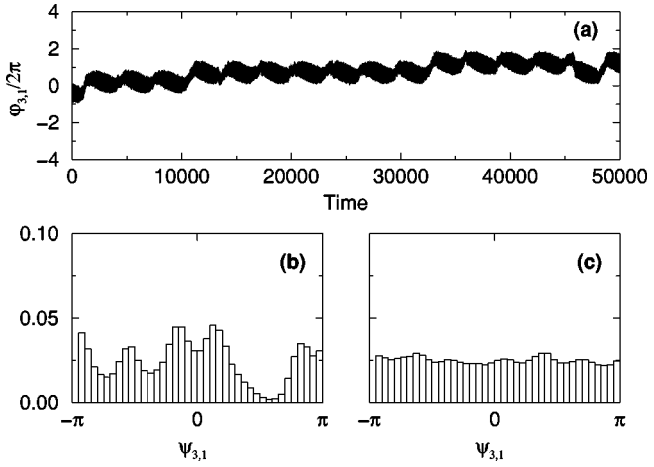

FIG. 9. Example of frequency locking without phase locking. In the case of modulation, the average frequency of the van der Pol oscillator is practically locked to that of the modulating force (a), but due to the presence of a second, subthreshold modulating term, the distribution of the cyclic relative phase is no longer unimodal (b). Noise makes this distribution practically uniform (c).

curs only if the amplitude of the modulation ε exceeds some threshold value (or at least the width of the synchronization region below this threshold is vanishingly small). The presence of noise smears the plateau in the $\Delta\Omega$ vs ν plot, as expected (Fig. 8, curve 2).

Now we add a second, *subthreshold*, modulating force so that $\mathcal{F}=0.6\sin\nu t+0.2\sin 0.307t$; the $\Omega=\langle\dot{\phi}_{vdP}\rangle$ vs ν plot still shows frequency locking (Fig. 8, curve 3). This *quasiperiodic modulation* was chosen here in order to simulate in a rough approximation the influence of two respiratory-related rhythms on the heart rate (see Sec. II). By this modulation the phase difference remains practically bounded [Fig. 9(a)]. Nevertheless, from Fig. 9(b) we see that within the synchronization region ($\varepsilon=0.6$ and $\nu=0.309$) the distribution of the cyclic relative phase is no longer unimodal; influence of noise makes this distribution practically uniform [Fig. 9(c)]. So, the quasiperiodic modulation shows an example of *frequency locking without phase locking*. (Another example is given in [44].)

It is important to underline the difference between synchronization and modulation. Due to modulation, the frequency Ω of an oscillator is not constant anymore, but changes from one cycle to another. If the modulation is, e.g., periodic with the frequency ν, then Ω also varies periodically, $\Omega(t)=\Omega_0+\tilde{\Omega}(\nu t)$, where $\tilde{\Omega}$ is a periodic function with the period $2\pi/\nu$. Exactly such a variation of the heart rate due to modulation by a respiratory-related rhythm is called RSA in the context of cardiorespiratory interaction. This variation may or may not be accompanied by the frequency locking, $n\langle\Omega\rangle=m\nu$, one of the effects that are studied in the present paper. Hence, RSA and cardiorespiratory synchronization are different, although definitely related phenomena. To speak of synchronization of the variation of the heart rhythm (variation of R-R intervals, or RSA) and respiration, as is done sometimes (cf. [45]), is not correct: the term modulation is more appropriate here.

To summarize the results of this section, the notion of synchronization in noisy systems is not unambiguous. Depending on the type of interaction, e.g., external forcing or modulation, one can observe either phase locking in the sense of Eq. (1) and locking of averaged frequencies, or phase locking in a statistical sense, i.e., existence of a preferred value of the cyclic relative phase Ψ [Eq. (2)] without frequency locking, or, finally, frequency locking and phase locking in the sense of Eq. (1), but without statistical preference of a certain value of Ψ.

IV. SYNCHRONIZATION APPROACH TO THE ANALYSIS OF BIVARIATE DATA

Now we discuss how the idea of synchronization can be used to study the underlying dynamics of possibly interacting complex systems from experimental data. A typical problem in time series analysis is to reveal the presence of an interdependence between two (or more) systems from the signals measured at their outputs. The analysis of these bivariate data is traditionally done by means of cross-correlation (cross-spectrum) technique [46] or nonlinear statistical measures like mutual information, maximal correlation, or bispectral analysis [47].

Recently, Schiff *et al.* [48] applied the mutual prediction technique to verify the assumption that measured bivariate data originate from two synchronized systems, where synchronization was understood as the existence of a functional relationship between the states of two systems, called generalized synchronization.

In our approach we assume that the measured bivariate data originate from two interacting self-oscillatory systems, which may either be phase synchronized or oscillate independently [18,40,43]. This means that we cannot consider the system under study as a ''black box,'' but need some additional knowledge to support this assumption in every particular case. For the study of cardiorespiratory interaction this assumption is quite reasonable; indeed, the cardiovascular and respiratory systems are individual oscillators having their own rhythms, but they are known to be coupled (see Sect. II). An advantage of our approach is that it allows us to address even weaker interaction between two oscillatory systems than that of Schiff *et al.* [48]. Indeed, the notion of phase synchronization implies only the existence of some relationship between phases, whereas the irregular amplitudes may remain uncorrelated. The irregularity of amplitudes can mask the phase locking so that traditional techniques treating not the phases but the signals themselves are less sensitive in the detection of systems' interrelation [18,49]. Moreover, the state of phase synchronization occurs for lower values of coupling than the state of generalized synchronization [17]; therefore, we expect it to be typical in natural systems, for instance, in cardiorespiratory interaction. Certainly, the relation between phases should be understood in a statistical sense [27,40,43].

Below we present several data-analysis techniques that reveal phase synchronization. Obviously, the first step in our analysis is the computation of the phases themselves. The *instantaneous phases* of an arbitrary signal can be obtained by means of the analytical-signal approach based on the Hilbert transform (see Appendix A). A very important property of this technique is that it does not require stationarity of the data. Sometimes, the signal can be reduced to a series of

events, i.e., to a point process. This is exactly the case in the analysis of cardiac activity, where the electrocardiogram is often reduced to the sequence of R peaks appearing at times t_i. Computation of the phase and frequency of such a process is described in Appendix B.

A. Analysis of phase difference

A straightforward approach to the analysis of synchronization is to plot the generalized phase difference $\varphi_{n,m}$ [see Eq. (1)] versus time and look for horizontal plateaus in this presentation; there exist no regular methods to pick up the integers n and m, so that they are usually found by trial and error. This simple method proved to be efficient in the investigation of model systems [15] as well as in some experimental data [18,49]. By means of $\varphi_{n,m}(t)$ plots one can trace transitions between synchronous and nonsynchronous states that are due to nonstationarity in interacting systems and/or coupling. A disadvantage of the method is that synchronous regimes that correspond to neighboring Arnold tongues, e.g., synchronization of orders $n:(m+1)$, appear in this presentation as nonsynchronous epochs. Respectively, in order to reveal all the regimes, one has to analyze a number of plots. Another drawback of this technique is that if noise is relatively strong, this method becomes ineffective and may be even misleading. Indeed, frequent phase slips mask the presence of plateaus (cf. Fig. 7) and synchronization can be revealed only by statistical approach, i.e., by analysis of the distribution of the cyclic relative phase $\Psi_{n,m}$.

For nonstationary data, such an analysis should be done in a running window; this approach turned out to be efficient for the analysis of synchronization between the activity of different brain areas as well as between brain and muscle activity from magnetoencephalography data [40].

B. Instantaneous frequency ratio

Another technique for the detection of synchronization is based on the analysis of the ratio of instantaneous frequencies of two signals (computation of these frequencies is described in the Appendices). For stationary data this ratio would be constant and would correspond to the winding (rotation) number.

As the precision of computation of frequencies for noisy data is rather poor, this method can be used only in addition to the analysis of phase differences. Its advantage is that there is no need to search for appropriate values of n and m; moreover, an approximately constant value of the ratio can be used for estimation of these integers. Besides, by analysis of instantaneous frequencies in nonstationary signals one can approach the question whether we indeed observe synchronization and not occasional coincidence of frequencies (see below).

C. Phase stroboscope: a synchrogram

The method presented here is closely related to the construction of a Poincaré section for a dynamical system. For example, a common way to study the dynamics of a periodically driven oscillator is to observe it stroboscopically with the period of the external force. Here we use a ''phase stroboscope,'' i.e., we observe the phase of one oscillator not

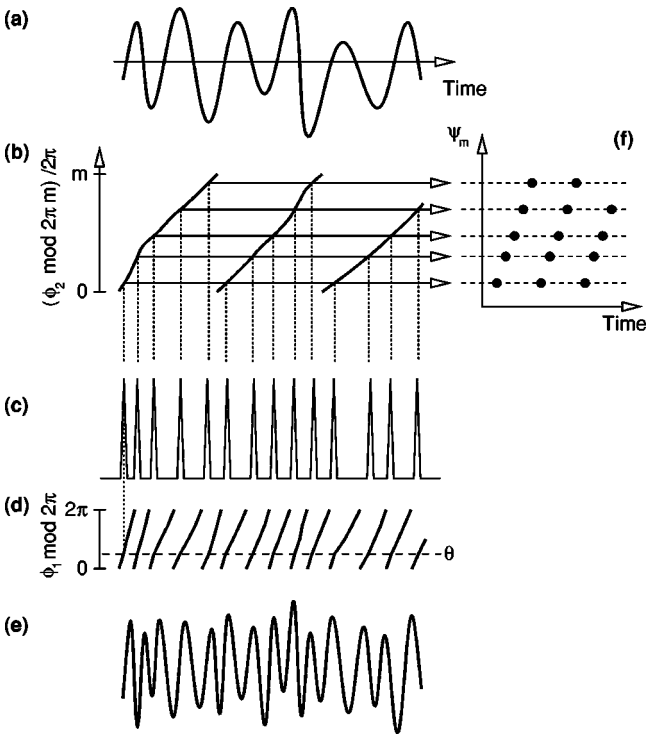

FIG. 10. Principle of the phase stroboscope, or synchrogram. Here a slow signal (a) is observed in accordance with a fast signal (e). Namely, it is observed when the cyclic phase (d) of the signal shown in (e) attains a certain fixed value θ (dashed line); these instants are marked by peaks shown in (c). Measured at these instants, the phase of the slow signal wrapped modulo $2\pi m$, (i.e., m adjacent cycles are taken as a one longer cycle) is plotted in (f); here $m=2$. In this presentation $n:m$ phase synchronization shows up as n horizontal lines. We note that if one signal, e.g., heartbeat, can be reduced to a point process, then the plot (c) is obtained in an obvious way.

periodically in time, but at times t_k when the cyclic phase of another one attains a certain fixed value θ, $\phi_1(t_k) \bmod 2\pi = \theta$, and construct a *synchrogram* by plotting $\psi(t_k)$ vs t_k, where

$$\psi(t_k) = \frac{1}{2\pi}[\phi_2(t_k) \bmod 2\pi]. \tag{5}$$

In the noise-free case of $n:1$ synchronization, the phase of the first oscillator attains the fixed value θ for n distinct values of ψ, so that this plot exhibits n horizontal lines. Noise smears out these lines, and some bands are expected to be observed instead.

It is important that this technique can be generalized to the case of $n:m$ synchronization by consideration of m adjacent oscillations of the second oscillator as one cycle (the phase within these cycles grows from 0 to $2\pi m$):

$$\psi_m(t_k) = \frac{1}{2\pi}[\phi_2(t_k) \bmod 2\pi m], \tag{6}$$

see Fig. 10. An important feature of this graphic tool is that, in contrast to phase difference plots, only one integer parameter m has to be chosen by trial. Moreover, several synchro-

nous regimes can be revealed within one plot, and the transitions between them can be traced. Indeed, if due to nonstationarity the coupled systems exhibit a transition from, e.g., 3:1 to 5:2 locking, then this is reflected in the proposed presentation with $m=2$ as a transition from a 6- to a 5-line structure; an example for our experimental data is presented in Sec. V A.

We stress two essential differences of this tool from those used in [21,24–26].

(i) For the construction of the plots we use for the y axis instantaneous phases instead of the time interval since the previous inspiration. This allows us (a) to address phase relations and to reveal phase-locking phenomena, i.e., to speak of synchronization in strict physical terms and (b) to deal with nonstationary data and neglect the variation of the respiratory period.

(ii) Wrapping the instantaneous phase that is defined on the whole real line into $[0,2\pi m]$ interval allows us to look for synchronous epochs of arbitrary order $n:m$ and not only $n:1$.

We note that if one of the signals, e.g., heartbeat, can be considered as a point process, then the natural way to choose the instants of the stroboscopic observation t_k is to take them as the instants of occurrence of characteristic events, e.g., R peaks in an ECG. In the context of the analysis of cardiorespiratory interaction, we call such plots cardiorespiratory synchrograms (CRS's) [27].

A very important property of the synchrogram is that it is equally effective in case of synchronization either by external or parametric forcing. On the contrary, the straightforward approach, i.e., the analysis of phase differences, is essentially less efficient in the case of parametric forcing, i.e., modulation. To illustrate this, we analyze a model example. Suppose the first signal is a pure sine wave, as an analogy to respiration, and the second one is a point process that imitates heartbeat. Let also 3 ''heartbeats'' occur within each ''respiratory'' cycle, i.e., 3:1 synchronization takes place. First we consider the case without modulation. Let the ''heartbeats'' occur at the following values of the ''respiratory'' phase: $\phi_r(t_k)=\phi_0+2\pi/3\cdot k$, where ϕ_0 is some constant and $k=0,1,2,\ldots$. The relative phase $\varphi_{3,1}$ at the times t_k when the ''heartbeats'' occur is, respectively, $\varphi_{3,1}(t_k)=3\phi_r-\phi_h=3(\phi_0+2\pi/3\cdot k)-2\pi\cdot k=3\phi_0$ and in the distribution of the cyclic relative phase $\Psi_{3,1}=\varphi_{3,1} \bmod 2\pi$ one observes a δ peak; in the presence of noise this peak is smeared. Now suppose that modulation takes place, i.e., ''heartbeats'' appear within each ''respiratory'' cycle with a nonuniform step:

$$\phi_r(t_k)=\begin{cases}\phi_0-\Delta+2\pi/3\cdot k, & k=0,3,6,\ldots\\ \phi_0+2\pi/3\cdot k, & k=1,4,7,\ldots\\ \phi_0+\Delta+2\pi/3\cdot k, & k=2,5,8,\ldots\end{cases}$$

Then, the relative phase attains three different values,

$$\varphi_{3,1}(t_k)=\begin{cases}3(\phi_0-\Delta),\\ 3\phi_0,\\ 3(\phi_0+\Delta),\end{cases}$$

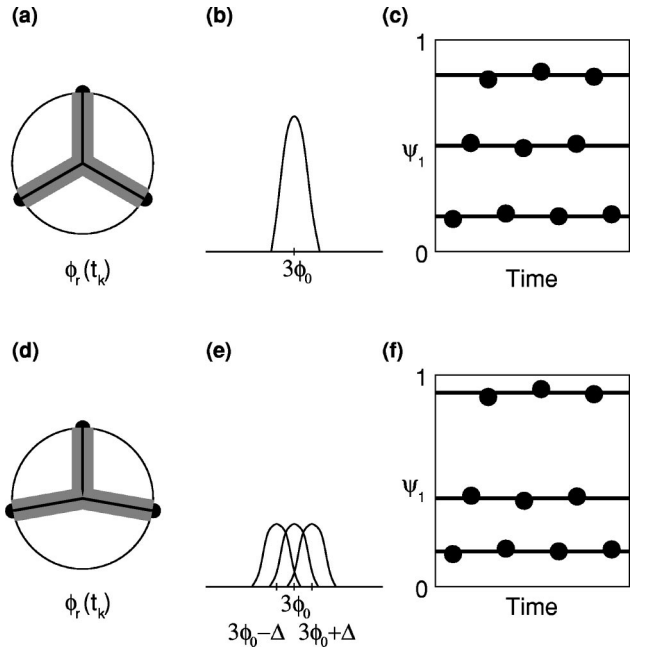

FIG. 11. Different efficiency of straightforward analysis of the relative phase and synchrogram technique in the case of synchronization via external forcing [(a), (b), and (c)] and modulation [(d), (e), and (f)]; 3:1 locking is taken here as an example. In the first case point events (''heartbeats'') occur at three equally spaced values of the ''respiratory'' phase (see text). These values are shown by black points on circle (a) and the corresponding radii. The noise smears these values; this is illustrated by the gray band around the radii. In this case, the distribution of the cyclic relative phase shows a single maximum (b). In the case of modulation, the events are not equally distributed on circle (d) and the respective distribution (e) has three maxima and is essentially broader than the one shown in (b). As a result, the synchronization seems to be not well expressed. Nevertheless, synchrograms (c) and (f) efficiently reveal synchronization in both cases. The difference between synchronization via external forcing or modulation shows up by different distances between the horizontal bands in these plots.

and the distribution of the cyclic relative phase has three peaks. Noise blurs these peaks so that they may overlap; nevertheless, the resulting distribution is rather broad if compared with the case without modulation. Hence, in this case, the analysis of the distribution is not reliable for the detection of synchronization. The synchrogram, on the contrary, demonstrates in both cases three bands and is, therefore, equally effective. The only difference is that these bands are either equally or nonequally spaced (Fig. 11).

V. DETECTING SYNCHRONIZATION BETWEEN HEART RATE AND RESPIRATION

In this section we describe the application of the above-presented methods to experimental data. We recall that respiratory signals are narrow-banded [cf. Fig. 1(b)], and, therefore, their phase and frequency can be computed by means of the Hilbert transform (see Appendix A); electrocardiograms [cf. Fig. 1(a)] can be reduced to point processes (sequences of R peaks) and treated as described in Appendix B. We present the details of our analysis for two subjects, and then summarize the results.

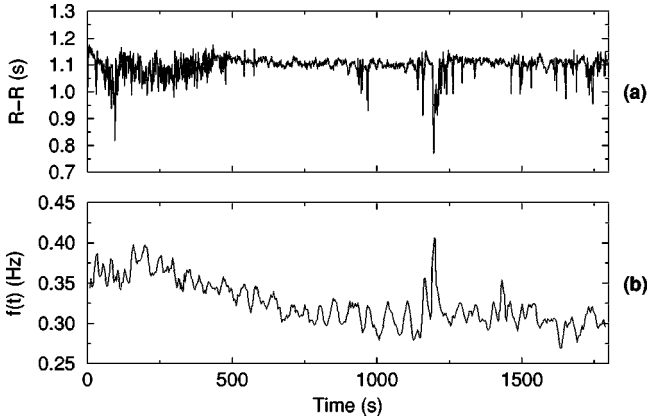

FIG. 12. The data for subject A: time course of R-R (interbeat) intervals (a) and of the instantaneous frequency $f(t)$ of respiration (b) clearly demonstrate the nonstationarity of the time series.

A. Example of phase locking

The sequence of R-R intervals and frequency of respiration for subject A (Fig. 12) clearly demonstrate the nonstationarity of the data. First, we analyze the generalized phase difference $\varphi_{n,m}$ for different values n and m and instantaneous frequency ratio (Fig. 13). The latter is an indication of the possibility of 5:2 locking within the first ≈ 300 s and of 3:1 locking appearing after ≈ 750 s. Nevertheless, from the analysis of relative phase only, we cannot reliably confirm the occurrence of synchronized epochs. Indeed, $\varphi_{3,1}$ exhibits some plateaus interrupted by phase slips only for the last 400 s (see inlet in Fig. 13); $\varphi_{5,2}$, as well as the values of relative phase for other locking ratios, displays no plateaus in this presentation.

The presence of 3:1 locking becomes more evident if we consider the distribution of the cyclic relative phase $\Psi_{3,1}$ [cf. Eq. (2)]. As the data are nonstationary, we compute this distribution in a running window (Fig. 14); the preference of a certain value of $\Psi_{3,1}$ within the last ≈ 900 s is clearly seen.

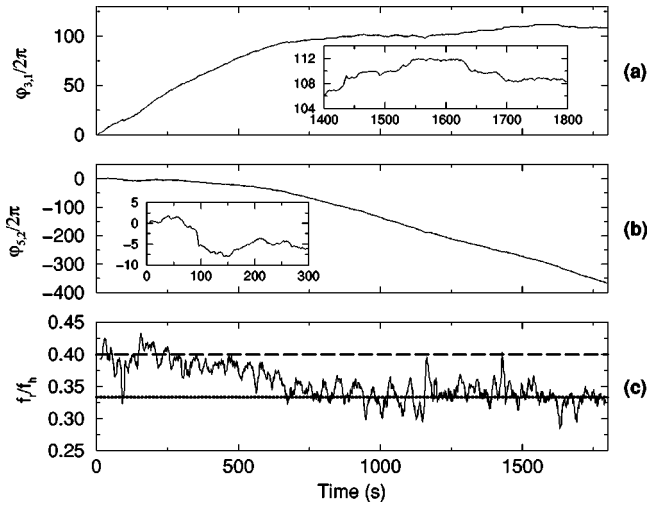

FIG. 13. Generalized phase difference and frequency ratio for subject A. Relative phase $\varphi_{3,1}$ (a) shows some indication of 3:1 phase locking. For a comparatively short period of time one can see plateaus in the plot of $\varphi_{3,1}$ vs time, interrupted by phase slips (see inlet). The time dependence of $\varphi_{5,2}$ (b) remains approximately constant during the first 300 s but displays no distinct plateaus, as can be seen from the zoomed plot (inlet). The instantaneous frequency ratio is shown in (c).

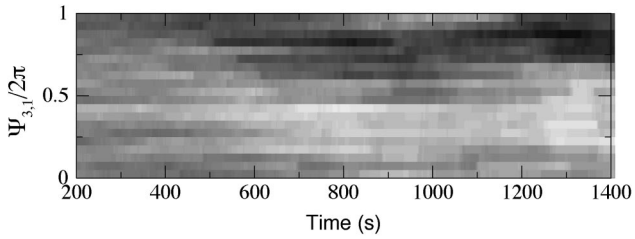

FIG. 14. Distribution of the cyclic relative phase $\Psi_{3,1}/2\pi$ calculated in a running window (400 heartbeats) and coded by gray scales also gives some indication of synchronization in the time interval 600–1400 s. Black color corresponds to the maximal values.

The next step is to perform the stroboscopic analysis of the respiratory phases as described in Section IV C. The CRS clearly exhibits six horizontal lines within the last ≈ 1000 s (Fig. 15); this is confirmed by the respective distribution (phase-density histogram) showing six well-expressed peaks. This presentation makes the presence of 3:1 phase locking in the data quite evident.

B. Example of frequency locking

Within the first ≈ 300 s the CRS for subject A (Fig. 15) has a clear 5-band structure. These bands are not horizontal;

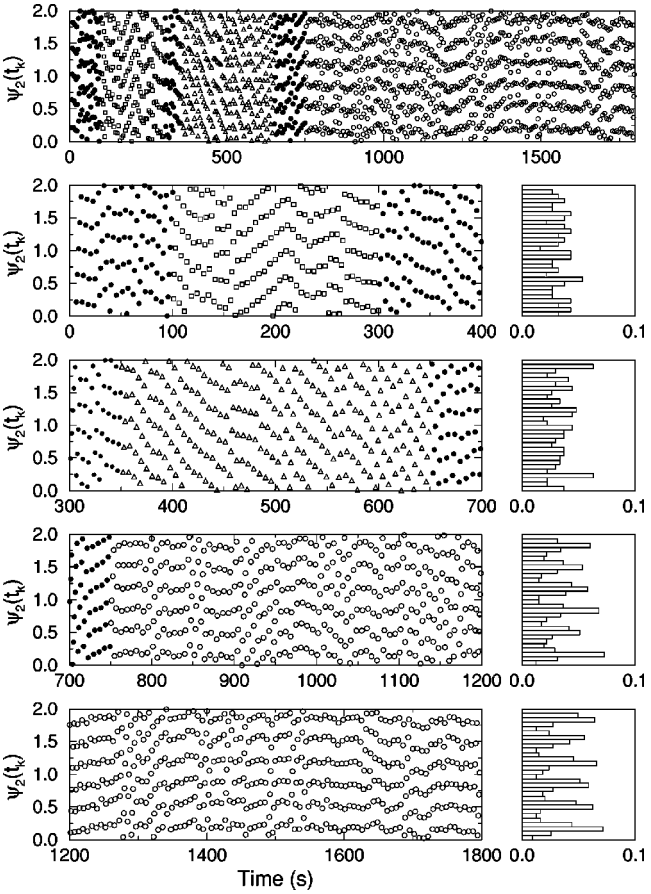

FIG. 15. (a) CRS of subject A, showing the transition from a 5-band structure (5:2 locking) to a 6-band structure (3:1 locking).

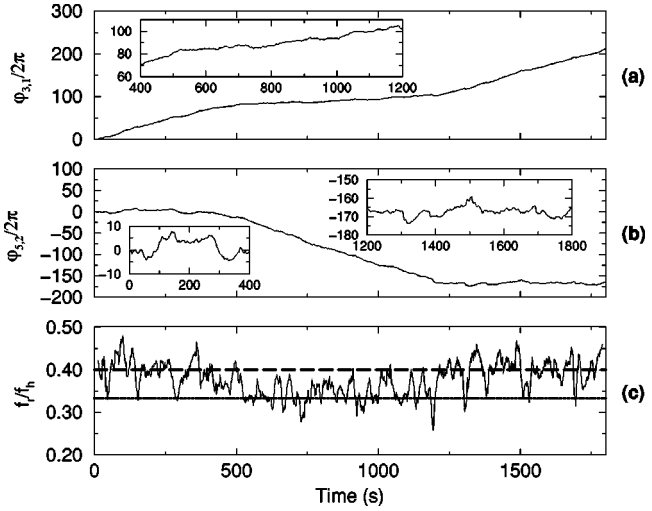

FIG. 16. Subject D. Relative phases $\varphi_{3,1}$ (a) and $\varphi_{5,2}$ (b) show some indication of 3:1 and 5:2 synchronization, respectively. This is consistent with the values of instantaneous frequency ratio (c). Although the plateaus in the time course of the relative phase are not very distinct [see inlets in (a) and (b)], statistically understood 3:1 phase locking can be confirmed by means of CRS (see Fig. 17). Note that within the last 600 s the generalized phase difference fluctuates around a constant level, indicating frequency locking on average.

hence, the distribution of ψ_2 is practically uniform, so that we cannot speak of phase locking. Nevertheless, the occurrence of these bands shows that, on average, two adjacent respiratory cycles contain 5 heartbeats, so that this epoch can be considered as an example of frequency locking.

Another illustrative example can be found in the data of subject D; these data were already introduced in Fig. 3. The analysis of relative phase and instantaneous frequency ratio (Fig. 16) indicates epochs of 3:1 and 5:2 synchronization. The CRS plot confirms that we encounter statistical 3:1 phase locking within the time interval $\approx 400-1200$ s (Fig. 17). The interval 1200–1800 s represents frequency locking; the relative phase $\varphi_{5,2}$ fluctuates around a constant value, so that, on average, the frequency ratio $f_h/f_r = 5:2$. Although we can find some short epochs with 5 distinct bands (e.g., around $t = 1400$ s), and the distribution of ψ_2 is not uniform, we cannot with confidence speak of phase locking in this case. From the other side, long-lasting coincidence of frequencies by pure chance seems to be very unlikely (compare with the model example in Sect. III A).

C. Summary of experimental results

The experimental results are summarized in Table II. The subjects are listed there in the order of ascending intensity of respiratory sinus arrhythmia. The latter is characterized in the following way. First we compute the RSA amplitude for every respiratory cycle as the difference between the longest and the shortest R-R interval within this cycle; if an R-R interval spans two neighboring cycles, it is considered to belong to that one, which contains more than 50% of the interval. Next, we calculate the median of the distribution of the RSA amplitude for all respiratory cycles; this quantity is taken as a measure of the RSA intensity.

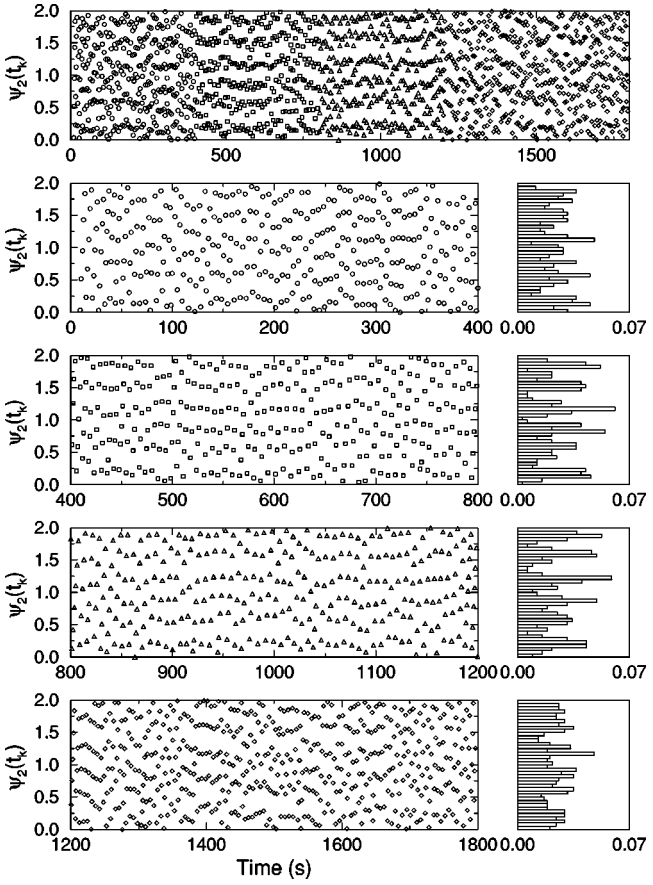

FIG. 17. (a) CRS of subject D demonstrates 6-band structure in the range 400–1200 s confirming 3:1 phase locking. Note that there is no phase locking in the statistical sense in those intervals where the generalized phase difference [Fig. 16(b)] indicates phase locking.

We observe that cardiorespiratory synchronization tends to become weaker with increasing RSA. Thus, these two effects might be the consequence of two competing physiological mechanisms. Another observation is that synchronization seems to be more pronounced in male subjects [50].

VI. DISCUSSION AND OUTLOOK

Concerning the interpretation of observed phase structures we have to be aware of an important issue: how can we be sure that these patterns of the relative phase indeed indicate synchronization, and, respectively, underlying nonlinear dynamics? How reliable is this indication? There is no straight way to answer these questions so far. Actually, as synchronization is not *a state, but a process* of adjustment of rhythms due to interaction, we cannot prove its existence if we do not have access to the system parameters and cannot check experimentally that the synchronous state is stable towards variation of the parameter mismatch within a certain range. As we are not able to do such experiments on humans, the only way to get some confirmation (but certainly not a proof) of our conclusions is to make use of the fact that the data are nonstationary. Indeed, we can trace the variation of the instantaneous frequencies of both signals and their relation. If we find some epochs, as in the case of our data, where both frequencies vary, but their relation remains stable

TABLE II. Summary of the results: the subjects are listed in the order of ascending amplitude of respiratory sinus arrhythmia; the amplitude of RSA is characterized by median and the interquartile range of the distribution of the RSA amplitude within every cycle (see text). The results show that synchronization and RSA seem to be competing phenomena. Note the indication of more pronounced synchronization in male subjects [50].

		RSA (s)		
Code	Sex	Median	IQR	Synchronization
A	m	0.015	0.040	3:1 (1000 s), 5:2 (300 s), 8:3 (20 s)
B	m	0.031	0.038	3:1 (several spells of 40 s)
C	m	0.046	0.057	3:1 (20 s), 7:2 (20 s), 4:1 (20 s)
D	f	0.056	0.057	5:2 and 3:1 (several spells of 30 s)
E	m	0.067	0.047	7:2 (60 s), 3:1 and 4:1 (20 s)
F	f	0.074	0.075	11:4 (20 s)
G	f	0.083	0.070	No synchronization detectable
H	f	0.264	0.296	No synchronization detectable

(Fig. 18), this can be considered as a strong indication in favor of our conclusion.

Another indication that also can be obtained using the fact of nonstationarity of the data is the presence of several different $n:m$ epochs within one record. Indeed, one can argue that observed phase or frequency locking of, e.g., order 3:1, could be due to the coincidence of frequencies of the uncoupled systems. Nevertheless, occasional coincidence of frequencies having the ratios exactly corresponding to neighboring Arnold tongues (3:1, 8:3, and 5:2 in case of subject A, cf. Fig. 19) seems to be very unlikely.

If the data are rather stationary and we are not able to find such epochs, the situation is more difficult. From the first sight, a natural way to address this problem is to use here the surrogate data techniques [51,25,40]. However, we see some serious problems in this approach. The usual formulation of the null hypothesis that is used for nonlinearity tests is to consider a Gaussian linear process [52] with a power spectrum that is identical to that of the tested signal; more sophisticated methods [53] imply also preservation of the probability distribution. Modification of this null hypothesis for the tests for synchronization—consideration of two surrogate signals that preserve the linear cross correlation between the original data—seems to be insufficient. Indeed, due to the definition of synchronization, we are interested in the relation between instantaneous phases, whereas the variations of amplitudes and their interrelation is of no importance. The usual way to construct surrogates (randomization of Fourier phases) used in [51] mixes the phase and amplitude properties transforming the variation of instantaneous phase into

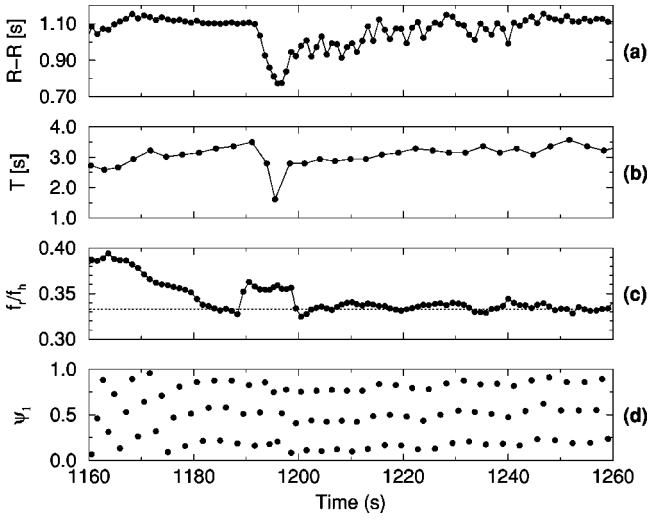

FIG. 18. A transient epoch within the data of subject A confirms the existence of synchronization. The periods of cardiac (R-R) and respiratory cycles (T) are shown in (a) and (b), respectively. After a short epoch of nonsynchronous behavior (1150–1200 s) the frequencies of heart rate and respiration change, probably due to the influence of a certain control mechanism, and become locked, i.e., $f_r/f_h \approx 1/3$. In the next 50 s we observe that, although both frequencies decrease, this ratio remains almost constant (c). This means that one of the systems follows the other one, i.e., synchronization takes place. 3:1 phase locking is also clearly seen from CRS (d).

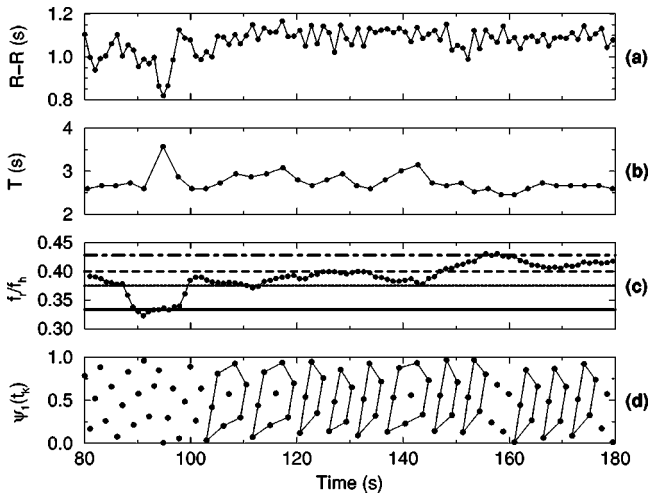

FIG. 19. Another transient epoch within the data of subject A. The periods of cardiac (R-R) and respiratory cycles (T) are shown in (a) and (b). The ratio of instantaneous frequencies (c) jumps between the values 1/3, 3/8, 2/5, and 3/7 corresponding to the neighboring synchronization regions; these values are shown by horizontal lines. Very short epochs of synchronization can be seen from the CRS (d) as several repeating patterns. So, e.g., the 8-point patterns mean 8:3 synchronization (8 different values of relative phase repeat themselves within 3 respiratory cycles).

the variation of instantaneous amplitude and vice versa. Besides, the signals generated by self-sustained oscillators possess certain properties of the distribution of instantaneous amplitudes (see [54] and references therein), and this distribution is destroyed by the Fourier phase randomization.

As a separate related problem, we mention quantification of synchronization strength. Two measures have been proposed to quantify statistical phase locking from the distribution of the relative phase [40]; the quantification of synchrograms remains an open question.

To conclude, although the general problem of reliability of estimates for the considered inverse problem requires further investigation, in the case of our experiments we can claim with high confidence that we have shown synchronization between the cardiovascular and the respiratory system in humans. In the present paper we have confirmed our earlier communication [27] that phases of both rhythms can be locked with different ratios $n:m$, and not only with $n:1$ as was shown in previous works. Our finding demonstrates that the cardiorespiratory interaction cannot be described in terms of ''triggering'' of one oscillator by another one [23].

From our time-series analysis we cannot directly draw a conclusion on the origin of coupling that is responsible for the effect we observe. Nevertheless, we can make the following remarks: (a) From the analysis of a transient epoch (Fig. 18) we see that first the heart rate remains practically constant while the frequency of respiration decreases. During this epoch the systems are not synchronized. Then, both rhythms accelerate abruptly, and synchronization sets in. This sudden change might be caused by the chemoreceptors signaling that the concentration of CO_2 in the blood increased due to slow breathing. Note that the onset of synchronization is accompanied by the appearance of RSA, i.e., by increased activity of some parts of the autonomous nervous system (ANS). Hence, in this particular case cardiorespiratory synchronization may be related to central neural regulation. (b) Preliminary results of the work in progress [55] show that synchronization can be also observed in heart transplant subjects. These subjects have no direct neural regulation of the heart rate by ANS; therefore, in this case, some other mechanisms are responsible for the locking phenomenon.

ACKNOWLEDGMENTS

We gratefully acknowledge valuable discussions with T. G. Anishchenko, V. S. Anishchenko, L. Glass, M. R. Guevara, N. B. Igosheva, M. C. Mackey, A. Pikovsky, P. Tass, and M. Zaks. The study was supported by the Deutsche Forschungsgemeinschaft (SFB 555). C.S. acknowledges financial support from the Max-Planck-Gesellschaft.

APPENDIX A: INSTANTANEOUS PHASE AND FREQUENCY OF A CONTINUOUS SIGNAL

A consistent way to define the phase of an *arbitrary* signal is known in signal processing as the analytic signal concept [56,46,57]. This general approach, based on the Hilbert transform (HT) and originally introduced by Gabor in 1946 [58,56], unambiguously gives the *instantaneous phase and amplitude* for a signal $s(t)$ via construction of the *analytic signal* $\zeta(t)$, which is a complex function of time defined as

$$\zeta(t)=s(t)+\imath\tilde{s}(t)=A(t)e^{\imath\phi(t)}, \tag{A1}$$

where the function $\tilde{s}(t)$ is the HT of $s(t)$,

$$\tilde{s}(t)=\pi^{-1}\mathrm{P}\int_{-\infty}^{\infty}\frac{s(\tau)}{t-\tau}d\tau \tag{A2}$$

and P means that the integral is taken in the sense of the Cauchy principal value. The instantaneous amplitude $A(t)$ and the instantaneous phase $\phi(t)$ of the signal $s(t)$ are thus uniquely defined from Eq. (A1).

As one can see from Eq. (A2), the HT can be considered as the convolution of the functions $s(t)$ and $1/\pi t$. Due to the properties of convolution, the Fourier transform $\tilde{S}(\omega)$ of $\tilde{s}(t)$ is the product of the Fourier transforms of $s(t)$ and $1/\pi t$. For physically relevant frequencies $\omega>0, \tilde{S}(\omega)=-\imath S(\omega)$. This means that the Hilbert transform can be realized by an ideal filter whose amplitude response is unity, and phase response is a constant $\pi/2$ lag at all frequencies [56].

An important advantage of the analytic signal approach is that the phase can be easily obtained from experimentally measured scalar time series. Numerically, this can be done via convolution of the experimental data with a precomputed characteristic of the filter (Hilbert transformer) [46,57,59]. Although HT requires computation on the infinite time scale, i.e., the Hilbert transformer is an infinite impulse response filter, the acceptable precision of about 1% can be obtained with the 256-point filter characteristic. The sampling rate must be chosen in order to have at least 20 points per average period of oscillation. In the process of computation of the convolution $L/2$ points are lost at both ends of the time series, where L is the length of the transformer. Alternatively, HT can be obtained by performing fast Fourier transform (FFT) of the original signal, shifting the phase of every frequency component by $-\pi/2$, and applying inverse FFT.

Although formally $A(t)$ and $\phi(t)$ can be obtained for an arbitrary $s(t)$, they have clear physical meaning only if $s(t)$ is a narrow-band signal, see the detailed discussion in [60]. In this case the amplitude $A(t)$ coincides with the envelope of $s(t)$, and the *instantaneous frequency* corresponds to the frequency of the maximum in the instantaneous spectrum.

Estimation of instantaneous frequency $f(t)$ of a signal is more cumbersome. Direct approach, i.e., numerical differentiation of $\phi(t)$, naturally results in very large fluctuations in the estimate of $f(t)$. Moreover, one may encounter that $f(t)<0$. This happens not only due to the influence of noise, but can result from a complicated form of the signal. For example, some characteristic patterns in the ECG (e.g., the T wave) result in negative values of instantaneous frequency. From a physical point of view, we expect that the instantaneous frequency is a slowly (with respect to the characteristic period of oscillations) varying positive function of time and has a meaning of a number of oscillations per time unit. This is especially important for the problem of synchronization where we are not interested in the behavior of the phase on a time scale smaller than the characteristic oscillation pe-

riod [16]. There exist several methods to obtain the estimates of $f(t)$ in accordance to this viewpoint; for a discussion and comparison, see [60].

Here we use the technique that is called in [60] a ''maximum likelihood frequency estimator.'' Suppose the instantaneous phase $\phi(t)$ is unwrapped into the infinite interval, so that this function is growing, although not necessarily monotonic. Then we perform for each instant of time a local polynomial fit on an interval essentially larger than the characteristic period of oscillations. The (analytically obtained) derivative of that polynomial function in this instant gives an estimate of the frequency that is always positive. Practically, we perform it by means of a Savitzky-Golay filter; a 4th-order polynomial and the interval of approximation equal approximately 10 characteristic periods seems to be a reasonable parameter choice. The instantaneous frequency computed in this way practically coincides with the maximum of running autoregression spectrum obtained, e.g., by means of the Burg technique [29], cf. Fig. 3.

APPENDIX B: PHASE AND FREQUENCY OF A POINT PROCESS

The series of R peaks can be considered as a sequence of point events taking place at times t_k. Phase and slowly varying frequency of such a process can be easily obtained. Indeed, the time interval between two R peaks corresponds to one complete cycle of the oscillatory process; therefore, the phase increase during this time interval is exactly 2π. Hence, we can assign to the times t_k the values of phase $\phi_k = \phi(t_k) = 2\pi k$. It is difficult to deal with this time series because it is not equidistantly spaced. Nevertheless, we can make use of the fact that it is a monotonically increasing function of time, and invert it. The resulting process $t(\phi_k)$ is equidistant, as the phase step is 2π. Now we can apply the polynomial fitting technique described in Appendix A to obtain the instantaneous period $T_k = T(\phi_k)$. Inverting the series once again we obtain the frequency $f_k = f(t_k) = 1/T_k$.

[1] A. Andronov, A. Vitt, and S. Khaykin, *Theory of Oscillations* (Gostekhizdat, Moscow, 1937) (in Russian), (Pergamon Press, Oxford, 1966) (in English); C. Hayashi, *Nonlinear Oscillations in Physical Systems* (McGraw-Hill, New York, 1964).

[2] R. L. Stratonovich, *Topics in the Theory of Random Noise* (Gordon and Breach, New York, 1963).

[3] I. I. Blekhman, *Synchronization of Dynamical Systems* (Nauka, Moscow, 1971) (in Russian); I. I. Blekhman, *Synchronization in Science and Technology* (Nauka, Moscow, 1981) (in Russian), (ASME Press, New York, 1988) (in English).

[4] P. S. Landa, *Nonlinear Oscillations and Waves in Dynamical Systems* (Kluwer Academic Publishers, Dordrecht, 1996).

[5] L. Glass and M. C. Mackey, *From Clocks to Chaos: The Rhythms of Life* (Princeton University Press, Princeton, NJ, 1988).

[6] B. van der Pol and J. van der Mark, Philos. Mag. **6**, 763 (1928).

[7] J. Aschoff, S. Daan, and G. Groos, *Vertebrate Circadian Systems. Structure and Physiology* (Springer, Berlin, 1982).

[8] G. A. Petrillo and L. Glass, Am. J. Physiol. **246**, 311 (1984).

[9] D. Bramble and D. Carrier, Science **219**, 251 (1983).

[10] J. Collins and I. Stewart, J. Nonlinear Sci. **3**, 349 (1993).

[11] J. Sturis *et al.*, Chaos **5**, 193 (1995).

[12] A. Neiman *et al.*, Phys. Rev. Lett. **82**, 660 (1999).

[13] V. S. Anishchenko *et al.* (unpublished).

[14] L. Glass, C. Graves, G. A. Petrillo, and M. C. Mackey, J. Theor. Biol. **86**, 455 (1980).

[15] M. G. Rosenblum, A. S. Pikovsky, and J. Kurths, Phys. Rev. Lett. **76**, 1804 (1996).

[16] A. S. Pikovsky, M. G. Rosenblum, G. V. Osipov, and J. Kurths, Physica D **104**, 219 (1997).

[17] M. G. Rosenblum, A. S. Pikovsky, and J. Kurths, Phys. Rev. Lett. **78**, 4193 (1997).

[18] M. G. Rosenblum, A. S. Pikovsky, and J. Kurths, IEEE Trans. Circuits Syst., I: Fundam. Theory Appl. **44**, 874 (1997).

[19] A. S. Pikovsky *et al.*, Phys. Rev. Lett. **79**, 47 (1997).

[20] H. Koepchen, in *Rhythms in Physiological Systems*, edited by H. Haken and H. Koepchen, Springer Series in Synergetics Vol. 55 (Springer, Berlin, 1991), pp. 3–20.

[21] K. Stutte and G. Hildebrandt, Pflugers Arch. Ges. Physiol. Menschen Tiere **289**, R47 (1966); P. Engel, G. Hildebrandt, and H.-G. Scholz, *ibid.* **298**, 258 (1968); H. Pessenhofer and T. Kenner, *ibid.* **355**, 77 (1975); T. Kenner, H. Pessenhofer, and G. Schwaberger, *ibid.* **363**, 263 (1976).

[22] F. Raschke, in *Temporal Disorder in Human Oscillatory Systems*, edited by L. Rensing, U. an der Heiden, and M. Mackey, Springer Series in Synergetics Vol. 36 (Springer-Verlag, Berlin, 1987), pp. 152–158.

[23] F. Raschke, in *Rhythms in Physiological Systems* (Ref. [20]), pp. 155–164.

[24] M. Schiek *et al.*, in *Nonlinear Analysis of Physiological Data*, edited by H. Kantz, J. Kurths, and G. Mayer-Kress (Springer, Berlin, 1998), pp. 191–209.

[25] H. Seidel and H. Herzel, IEEE Eng. Med. Biol. Mag. **17**, 54 (1998).

[26] H. Seidel, Ph.D. thesis, TU Berlin, 1998.

[27] C. Schäfer, M. G. Rosenblum, J. Kurths, and H.-H. Abel, Nature (London) **392**, 239 (1998).

[28] R. Schmidt and G. Thews, *Human Physiology* (Springer, New York, 1983).

[29] W. H. Press, S. T. Teukolsky, W. T. Vetterling, and B. P. Flannery, *Numerical Recipes in C*: *the Art of Scientific Computing*, 2nd ed. (Cambridge University Press, Cambridge, England, 1992).

[30] J. Saul, in *Rhythms in Physiological Systems* (Ref. [20]), pp. 115–126.

[31] G. Anrep, W. Pascual, and R. Rössler, Proc. R. Soc. London, Ser. B **119**, 191 (1936).

[32] C. Davies and J. Neilson, J. Appl. Physiol. **22**, 947 (1967).

[33] D. Eckberg, Y. Kifle, and V. Roberts, J. Physiol. (London) **304**, 489 (1980).

[34] M. Gilbey, D. Jordan, D. Richter, and K. Spyker, J. Physiol. (London) **356**, 65 (1984).

[35] H. Koepchen, P.-H. Wagner, and H. Lux, Pflugers Arch. Ges.

Physiol. Menschen Tiere **273**, 443 (1961).

[36] I. I. Blekhman, P. S. Landa, and M. G. Rosenblum, Appl. Mech. Rev. **48**, 733 (1995).

[37] We note that sometimes definition (1) is understood in a very narrow sense $|n\phi_1 - m\phi_2| = \text{const}$ that is only valid for quasiharmonic oscillations and excludes, e.g., the obvious case of synchronization of two relaxational oscillators and other nontrivial phenomena.

[38] P. S. Landa, *Self-Oscillations in Systems with Finite Number of Degrees of Freedom* (Nauka, Moscow, 1980) (in Russian).

[39] M. G. Rosenblum, A. S. Pikovsky, and J. Kurths, in *Stochastic Dynamics*, edited by L. Schimansky-Geier and T. Pöschel, Lecture Notes in Physics Vol. 484 (Springer, Berlin, 1997), pp. 233–244.

[40] P. Tass *et al.*, Phys. Rev. Lett. **81**, 3291 (1998).

[41] The phase of a chaotic oscillator can be determined by means of three different approaches, see [16]. Suppose we can define a Poincaré map for the autonomous continuous-time system. Then, we define the phase proportional to time between two cross sections with the Poincaré surface so that the phase increment is 2π at each rotation, $\phi(t) = 2\pi(t - t_n)/(t_{n+1} - t_n) + 2\pi n$ and $t_n \leqslant t < t_{n+1}$, where t_n is the time of the nth crossing of the secant surface. Quite often it is possible to find such a projection of a strange attractor that the phase portrait looks like rotations around some origin. In this case the phase can be determined as the angle between the projection of the phase point on the plane and a given direction on the plane. Finally, the phase of a properly chosen oscillatory observable computed via Hilbert transform, can be taken as the phase of the chaotic oscillator. Note that although the phases determined by different techniques often do not coincide microscopically, i.e., on a time scale less than the average period of oscillation, they have equal average growth rates. In other words, the mean frequencies defined as the average of $d\phi/dt$ over a large period of time, coincide.

[42] Indeed, the heart rate is always several times larger than the frequency of respiration; therefore, the choice of the frequency ratio $n:m = 3:1$ for the purposes of illustration is reasonable; this is confirmed by experimental results presented in Sec. V.

[43] M. Rosenblum *et al.*, IEEE Eng. Med. Biol. Mag. **17**, 46 (1998).

[44] C. Schäfer, Ph.D. thesis, Potsdam University, 1998.

[45] D. Hoyer *et al.*, in *Nonlinear Analysis of Physiological Data* (Ref. [24]), pp. 167–190.

[46] L. Rabiner and B. Gold, *Theory and Application of Digital Signal Processing* (Prentice-Hall, Englewood Cliffs, NJ, 1975).

[47] A. Rényi, *Probability Theory* (Akadémiai Kiadó, Budapest, 1970); B. Pompe, J. Stat. Phys. **73**, 587 (1993); H. Voss and J. Kurths, Phys. Lett. A **234**, 336 (1997); S. Zhong, G. Gebber, S.-Y. Zhou, and S. Barman, Am. J. Physiol. **275**, H331 (1998).

[48] S. Schiff *et al.*, Phys. Rev. E **54**, 6708 (1996).

[49] M. G. Rosenblum, G. I. Firsov, R. Kuuz, and B. Pompe, in *Nonlinear Analysis of Physiological Data* (Ref. [24]), pp. 283–306.

[50] This observation was made by T. G. Anishchenko (private communication). This fact might be explained by age and gender differences in heart rate variability. Indeed, for young persons the latter is more pronounced in women, see K. Jensen-Urstad *et al.*, Acta Physiol. Scand. **160**, 235 (1997); P. K. Klein, R. E. Kleiger, and J. N. Rottman, Am. J. Cardiol. **80**, 302 (1997); due to the reduced sympathetic influence that is known to decrease the heart rate variability, see Yu. A. Khramov and B. P. Veber, Fiziol. Chel. **11**, 911 (1985); A. V. Ng, R. Callister, D. G. Johnson, and D. R. Seals, Hypertension (Dallas) **21**, 498 (1993).

[51] M. Palus, Phys. Lett. A **227**, 301 (1997).

[52] J. Theiler *et al.*, Physica D **58**, 77 (1992); J. Kurths and H. Herzel, *ibid.* **25**, 165 (1987).

[53] T. Schreiber and A. Schmitz, Phys. Rev. Lett. **77**, 635 (1997).

[54] M. F. Dimentberg, *Nonlinear Stochastic Problems of Mechanical Oscillations* (Nauka, Moscow, 1980) (in Russian); P. Landa and A. Zaikin, Phys. Rev. E **54**, 3535 (1996).

[55] E. Toledo *et al.*, *Proceedings of the International Symposium on Nonlinear Theory and its Applications* (Presses Polytechniques et Universitaires Romandes, Lausanne, 1998), Vol. 1, pp. 171–174.

[56] P. Panter, *Modulation, Noise, and Spectral Analysis* (McGraw-Hill, New York, 1965).

[57] M. Smith and R. Mersereau, *Introduction to Digital Signal Processing. A Computer Laboratory Textbook* (Wiley, New York, 1992).

[58] D. Gabor, J. IEE London **93**, 429 (1946).

[59] J. Little and L. Shure, *Signal Processing Toolbox for Use with MATLAB. User's Guide* (Mathworks, Natick, MA, 1992).

[60] B. Boashash, Proc. IEEE **80**, 520 (1992).